Title

A Fulvic Acid-like Substance Participates in the Pro-inflammatory Effects of Cigarette Smoke and Wood Smoke Particles

Journal

Chemical Research in Toxicology, 33(4)

ISSN

0893-228X

Authors

Gonzalez, David H
Soukup, Joleen M
Madden, Michael C
et al.

Publication Date

2020-04-20

DOI

10.1021/acs.chemrestox.0c00036

Peer reviewed

Published in final edited form as:
Chem Res Toxicol. 2020 April 20; 33(4): 999–1009. doi:10.1021/acs.chemrestox.0c00036.

A fulvic acid-like substance participates in the pro-inflammatory effects of cigarette smoke and wood smoke particles

David H. Gonzalez[1], **Joleen M. Soukup**[2], **Michael C. Madden**[2], **Michael Hays**[2], **Jon Berntsen**[3], **Suzanne E. Paulson**[1], **Andrew J. Ghio**[2]

[1]Atmospheric and Oceanic Sciences, University of California at Los Angeles, CA 90095

[2]US Environmental Protection Agency, Research Triangle Park NC 27711

[3]TRC Environmental, Chapel Hill, NC 27599

Abstract

We tested the postulate that 1) a fulvic acid (FA)-like substance is included in cigarette smoke and wood smoke particle (WSP) and 2) cell exposure to this substance results in a disruption of iron homeostasis associated with a deficiency of the metal and an inflammatory response. The fluorescence excitation-emission matrix spectra of the water-soluble components of cigarette smoke condensate and WSP (Cig-WS and Wood-WS) approximated those for the standard reference materials, Suwanee River and Nordic fulvic acids (SRFA and NFA). Fourier transform infrared (FT-IR) spectra for the FA fraction of cigarette smoke and WSP (Cig-FA and Wood-FA), SRFA and NFA also revealed significant similarities (O-H bond in alcohols, phenols or carboxylates, C=O in ketones, aldehydes and carboxylates, and a significant carboxylate content). After exposure to Cig-WS and Wood-WS and the FA standards, iron was imported by respiratory epithelial cells reflecting a functional iron deficiency. The release of pro-inflammatory mediators interleukin (IL)-8 and IL-6 by respiratory epithelial cells also increased following exposures to Cig-WS, Wood-WS, SRFA, and NFA. Co-exposure of the respiratory epithelial cells with iron decreased supernatant concentrations of the ILs relative to exposures to Cig-WS, Wood-WS, SRFA and NFA alone. It is concluded that 1) FA-like substance is included in cigarette smoke and WSP and 2) respiratory epithelial cell exposure to this substance results in a disruption of iron homeostasis associated with both a cell deficiency of the metal and inflammatory response.

Graphical Abstract

Correspondence should be addressed to: Andrew Ghio, Human Studies Facility, 104 Mason Farm Road, Chapel Hill, NC 27599, Telephone #: (919)-966-0670; FAX #: (919)-966-6271; ghio.andy@epa.gov.

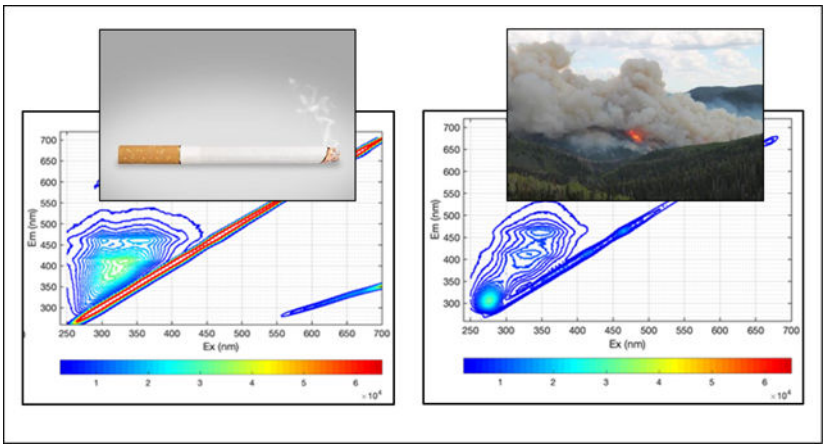

Keywords

Fulvic acid; smoking; air pollution; iron; lung diseases; inflammation

Introduction

HUmic-LIke Substances (HULIS) are a mixture of water-soluble, complex, organic, macromolecular compounds that have been identified in fog, cloud water, biomass burning aerosol, wood smoke, and cigarette smoke.[1–7] HULIS are thought to participate in the inhalation toxicity of cigarette smoke and wood smoke particle (WSP), but this role is not well defined.[1,8,9] The toxic properties of HULIS may result from the high content of oxygenated functional groups (ketones, carboxylates and phenolates) that form stable complexes with transition metals, in particular with iron (Fe).[1,8,10–12] HULIS is a component of cigarette smoke believed to be in the fraction that binds transition metals.[13] The ability of HULIS to chelate Fe has been associated with reactive oxygen species (ROS) generation and functional deficiency of cellular Fe that leads to transcription factor activation and release of proinflammatory mediators and tissue injury.[1,7,9,14] HULIS derived from biomass burning has been associated with significantly higher optical absorption and ROS activity in simulated lung fluids relative to HULIS formed from atmospheric processing.[15]

HULIS has also been identified in cigarette smoke and lung tissues of smokers, and has been shown to produce ROS, accumulate Fe, and induce collagen deposition, suggesting that Fe binding by these substances plays a role in lung injury after inhalation of particulate matter (PM).[1] Cigarette smoke-derived HULIS introduced into the lungs of an animal model is phagocytosed and leads to an intracellular accumulation of Fe.[1] Exposure of BEAS-2B (respiratory epithelial) cells to WSP increased cellular ROS generation, sequestration of mitochondrial Fe, mitogen-activated protein kinase activation, nuclear factor erythroid 2-related factor 2 (NRF2) transcription activation, and release of interleukin (IL)-6 and IL-8 proinflammatory mediators.[9] These effects were considered the result of exposure to HULIS in the WSP; suggesting that HULIS in the lung complexes host cellular Fe causing a functional Fe deficiency and inducing a cascade of proinflammatory events that may

manifest as lung injury.[9] HULIS mediated disruption of cellular Fe homeostasis was postulated to be a common pathway for pulmonary and systemic health effects arising from exposure to cigarette smoke, biomass burning aerosols, and ambient urban PM. These studies suggest an ability of HULIS to bind Fe and initiate detrimental health effects. Accordingly, some of the effects of cigarette smoke and WSP on human health can result from an inclusion of HULIS in both.

HULIS derives its name from its physical and chemical similarities to terrestrial and aquatic humic substances.[4] Traditionally, soil humic substances have been extracted at alkaline pH to separate an insoluble material, referred to as humin. Acidification of the alkaline extract to pH 1 produces a precipitant that is defined as the humic acid (HA) fraction and the remaining supernatant is the fulvic acid (FA) fraction.[4] Thus, the fractions of soil humic substances are operationally defined as humin (insoluble), HA (alkaline soluble) and FA (soluble at all pH values). A variety of gel permeation chromatography methods have been developed to remove inorganic impurities and concentrate fractions of humic substances.[4] Early studies on atmospheric HULIS have used alkaline extraction and gel permeation chromatography methods to study both the soluble and insoluble components.[16–18] Recent studies have focused on the water-soluble fraction of ambient HULIS that, by definition, is more similar to FA.[4]

Spectroscopic characterization has revealed that HULIS shares numerous functional groups with HA and FA, including carboxylic and phenolic groups, but HULIS generally has weaker acid characteristics, lower molecular weight and aromaticity and higher aliphatic character.[4,19] Fluorescence characterization of HULIS has been used to identify fluorophores that bear similarities to those in HA and FA.[4,19] Two distinct excitation/emission peaks (ex/em) have been identified in HULIS, a FA-like ex/em pair at 330–350 nm/420–480 nm and a HA-like ex/em pair at 250–260 nm/380–480 nm.[20] HULIS from PM and fog water have shorter wavelength fluorescence peaks when compared to soil humic substances.[21,22] This has been attributed to a lower aromatic content and higher condensed conjugated bonds and aliphatic character in HULIS.[21,22]

Fourier transform infrared (FT-IR) spectroscopy is a useful tool for characterizing HULIS as it reveals information on organic functional groups. HA, FA and HULIS all share several similar FT-IR peaks, yet differences in HULIS have been identified.[4,19] Generally, these FT-IR spectra reveal broad absorption peaks centered around 3300 cm^{-1} (O-H stretch from alcohols, phenols and carboxylic acids), 2960–2860 cm^{-1} (C-H stretch from aliphatic), 1720 cm^{-1} (C=O stretch mostly from carboxylic acids), 1600–1660 cm^{-1} (C=C stretch from aromatics and C=O stretches from conjugated carbonyls), around 1400 cm^{-1} (a broad peak; C-H stretch aliphatics), and 1220 cm^{-1} (C=O stretch and O-H bending from carboxylates) and a pair of peaks ranging from 2970–2840 cm^{-1} and 3030 cm^{-1} (C-H stretch from aliphatics).[18,22–24] However, HULIS samples have shown relatively strong discrete peaks at 1589 cm^{-1}, 1280 cm^{-1} and 863 cm^{-1}, indicating organic nitrate groups (R-ONO_2) that are not found in soil humic substances.[24] These peaks have also been identified in humic substances.[24] No standard HULIS material exists, but due to the similarity of functional groups, solubility and molecular weight several studies have used FA (usually Suwannee River Fulvic Acid; SRFA) as a HULIS surrogate.[4,25,26]

In this work we tested the postulate that 1) a FA-like substance is included in cigarette smoke and WSP and 2) the FA-like substance in cigarette smoke and WSP participates in the biological effects following their exposure by disrupting cell iron homeostasis. We use fluorescence and FT-IR spectroscopy to characterize HULIS in the water-soluble fraction of cigarette smoke (Cig-WS), the water-soluble fraction of wood-smoke particle (Wood-WS) and SRFA. Using a traditional alkaline extraction method, we isolate the FA fraction of HULIS from cigarette smoke (Cig-FA) and wood-smoke particle (Wood-FA). We then use fluorescence and FT-IR spectroscopy to characterize Cig-FA and Wood-FA and compare it to their water-soluble counterparts and SRFA. Fluorescence excitation-emission matrix (EEM) and FT-IR spectroscopy are used to compare fluorophores and organic functional groups present among the different samples.

Experimental procedures

Materials.

All reagents were from Sigma Co. (St. Louis, MO) unless specified otherwise. SRFA (Standard II) and Nordic fulvic acid (NFA, reference) were obtained from the International Humic Substances Society (IHSS; St. Paul, MN).

Cigarette smoke condensate (CSC) was obtained from the Tobacco Health Research Institute, University of Kentucky. Preparation from the mainstream smoke from Kentucky Reference 1R1 cigarettes was automated and has been previously described.[27] Water-soluble extract of cigarette smoke (Cig-WS) was prepared by agitating 10 mg CSC/1.0 mL Hank's buffered saline solution (HBSS) for 2 hr, centrifugation of the suspension at 10000 G x 10 minutes, and separating the supernatant.

WSP was generated by heating white oak wood on an electric heating element (Brinkmann Corporation, Dallas, TX) in a Quadrafire 3100 woodstove (Colville, WA). WSP was collected by bubbling the smoke through 100% ethanol. The resulting suspension was treated in both a SpeedVac Concentrator (Savant, Life Technologies Corporation, Grand Island, NY) and a lyophilizer (Labconco, Fort Scott, KS). The ratio of elemental to organic carbon in the final WSP was 0.004 ± 0.002 (Sunset Labs, Hillsborough, NC) suggesting elemental carbon comprises approximately 0.4% of the WSP. Diluted WSP was injected into a gas chromatograph (Gerstel Thermal Desorption System/Agilent 6890 equipped with an Agilent 5973 mass selective detector).[28] Similar to prior studies, identifiable compounds included levoglucosan (25.3%, mass/mass), syringealdehyde (10.3%), 4-hydroxy-3-methoxy cinnamaldehyde (3.2%), 3,5-dimethoxy-4-hydroxyacetophenone (1.7%), vanillin (0.8%), isoeugenol (0.6%), ethylguaiacol <0.1%), guaiacol (<0.1%), 2-methxoymethylphenol (<0.1%), eugenol (<0.1%), and propylguaiacol (<0.1%).[29] A water-soluble extract of WSP (Wood-WS) was prepared by agitating 10 mg particle/1.0 mL HBSS for 2 hr, centrifugation of the suspension at 10000 G x 10 minutes and separating the supernatant.

To isolate the FA faction of cigarette smoke and WSP (Cig-FA and Wood-FA), the alkaline extraction procedure was used. Briefly, CSC and WSP were brought to pH 13 using 1 M NaOH and centrifuged at 10000 G x 10 minutes. The resulting supernatant was acidified to pH 1 using HCl and centrifuged at 10000 G x 10 minutes, separating the supernatant. The

resulting Cig-FA and Wood-FA was brought to a pH of 5.5–6.0 using 1 M NaOH and then stored in a freezer (0° C) until analysis.

Fluorescence and FT-IR Analysis of Materials.

Fluorescence excitation-emission matrix (EEM) scans were performed on all samples using a Lumina Spectrometer, (Thermo Scientific). Fluorescence EEM spectra covering λ_{ex} = 250–700 nm and λ_{em} = 255–705 nm in 5 nm intervals at a scan speed of 60 nm/min were obtained. Fluorometer parameters included an ex/em slit size of 10 nm and an integration time of 10 ms. Fluorescence analysis was performed on the aqueous solutions of Cig-WS, Wood-WS, Cig-FA, Wood-FA and SRFA. In all fluorescence EEM spectra, the diagonal line across spectra is an instrument artifact due to Rayleigh scattering.[30]

FT-IR scans were performed on Cig-FA, Wood-FA and SRFA using a UATR Two FT-IR spectrometer (Perkin-Elmer, Norwalk, CT). In order to minimize solvent interferences, Cig-FA and Wood-FA samples were evaporated to dryness with a gentle stream of N_2 at room temperature. SRFA was analyzed as a solid, as received from IHSS. NFA FT-IR data is provided by IHSS.

Cell culture.

BEAS-2B cells, an immortalized line of normal human bronchial epithelium, were employed for *in vitro* investigations. Cells were grown to 90–100% confluence on uncoated plastic twelve-well plates in keratinocyte growth medium (KGM; Clonetics, Walkersville, MD) which is essentially MCDB 153 medium supplemented with 5 ng/ml human epidermal growth factor, 5 mg/ml insulin, 0.5 mg/ml hydrocortisone, 0.15 mM calcium, bovine pituitary extract, 0.1 mM ethanolamine and 0.1 mM phosphoethanolamine. Using release of lactic dehydrogenase and trypan blue exclusion as endpoints, there was no significant cytotoxicity with 24 hr exposure to 100 μL Cig-WS, 100 μL Wood-WS, 100 μg/mL SRFA, and 100 μg/mL NFA.

Cell iron concentrations.

BEAS-2B cells were exposed to 100 μL Cig-WS, 100 μL Wood-WS, 100 μg/mL SRFA, or 100 μg/mL NFA in media for 4 hr. After removal of the Cig-WS, Wood-WS, SRFA, and NFA, the media was replaced, and cells were exposed to 200 μM ferric ammonium citrate (FAC) for 4 hr incubation. After completion of the incubation, the media was removed and the cells were washed with HBSS and scraped into 1.0 mL 3 N HCl/10% trichloroacetic acid (TCA). After hydrolysis at 70° C for 24 hr with precipitation of heme in the 10% TCA, iron (non-heme) concentration in the supernatant was determined at λ=238.204 nm using inductively coupled plasma optical emission spectroscopy (ICPOES; Model Optima 4300D, Perkin Elmer).

Cell ferritin concentrations.

BEAS-2B cells were exposed to 100 μL Cig-WS, 100 μL Wood-WS, 100 μg/mL SRFA, or 100 μg/mL NFA in media for 4 hr. FAC was added to a final concentration of 200 μM and the incubation continued for 24 hr. After the media was removed, cells were washed with HBSS, scraped into 1.0 mL HBSS, and disrupted using five passes through a gauge 25

needle. The concentrations of ferritin in the lysates were quantified using an immunoturbidimetric assay (Kamiya Biomedical Company, Seattle, WA).

IL-6 and IL-8 release.

BEAS-2B cells were exposed to 100 μL Cig-WS, 100 μL Wood-WS, 100 μg/mL SRFA, or 100 μg/mL NFA in media for 4 hr. FAC was added to a final concentration of 200 μM and the incubation continued for 24 hr. IL-6 and IL-8 concentrations in cell media were measured using enzyme linked immunosorbent assay (ELISA) methodology (R&D Systems, Minneapolis, MN).

Statistics.

Data are expressed as mean values ± standard deviation (SD) unless specified otherwise. The minimum number of replicates for all cellular and protein measurements was nine unless specified otherwise. Differences between multiple groups were compared using one-way analysis of variance; the post-hoc test employed was Tukey's range test. Two-tailed tests of significance were employed. Significance was assumed at $p < 05$.

Results

Fluorescence EEM spectra.

Figure 1 shows the fluorescence EEM spectra of 30 μg/mL aqueous SRFA and NFA. SRFA shows two distinct fluorescence peaks centered at ex/em = (325–350) nm/(460–465) nm and ex/em = (320–325) nm/420 nm. NFA has markedly different EEM features than SRFA, with two distinct fluorescence peaks centered at ex/em = 410 nm/(470–475) nm and ex/em 455 nm/(500–545) nm. The reasons for this are not known.

The fluorescence EEM spectrum of Cig-WS and the Cig-FA are shown in Figure 2. Cig-WS was diluted to a final concentration of 5.4 μg/mL to avoid signal saturation and related red shifting of fluorescence contours. Cig-FA was diluted by 100×, but the mass concentration of Cig-FA is not known. Both Cig-WS and Cig-FA have very similar fluorescence EEM, with two sets of distinct peaks at ex/em = (340–355) nm/460 nm and ex/em = (325–350) nm/(415–420) nm. These peaks are similar to the fluorescence peaks observed for SRFA EEM (Fig. 1). This indicates that the bulk if not all of Cig-WS is composed of Cig-FA with fluorophores resembling those of SRFA. However, both Cig-WS and Cig-FA EEMs (Fig. 2) have contours stretching into lower wavelengths, features not observed in SRFA EEM.

The fluorescence EEM spectra for 5.4 μg/mL Wood-WS and Wood-FA are shown in Figure 3. Wood-FA was diluted by 50×, but the mass concentration is not known. The fluorescence EEM of Wood-WS and Wood-FA show strikingly different features (Figure 3). Wood-WS exhibits two peaks at ex/em = 410 nm/465 nm and ex/em = 455 nm/(515–550) nm, nearly identical to fluorescence features of NFA (Figure 1). The Wood-FA fraction shows two distinct peaks at ex/em = (320–350) nm/(405–420) nm and ex/em = 345–355 nm/(460–465) nm that resemble those of SRFA, Cig-WS and Cig-FA. The differences in EEM features indicate that the dominant fluorophores in Wood-WS are markedly different than the Wood-FA fraction. Interestingly, the Wood-FA fraction shows a third distinct peak centered at

ex/em = 275 nm/(300–320) nm not observed in Cig-WS, Cig-FA, SRFA or NFA. This could be due to the presence of single oxygenated aromatic molecules, such as phenols and methoxyphenols, that are commonly associated with the water-soluble fraction of WSP.[29] Interestingly, none of the EEM exhibited the commonly reported HA-like ex/em pair at 250–260 nm/380–480 nm.[20]

FT-IR spectra.

FT-IR spectra of solid Cig-FA, Wood-FA and SRFA are shown in Figures 4A and 4B. Common FT-IR absorbances and functional groups between Cig-FA, Wood-FA, SRFA, NFA are summarized in Table 1. All FT-IR spectra exhibit several striking similarities. All samples have a broad peak near 3300–3400 cm^{-1} indicating O-H stretching in alcohols, phenols or carboxylates. Peaks centered near 2938–2975 cm^{-1} indicate C-H stretching from aliphatic groups. Another infrared absorption of interest is the peak at 1707–1727 cm^{-1} characteristic of C=O stretching from carboxylates and to a lesser degree ketones and aldehydes.[22,24] All samples have somewhat broad peaks centered around 1615 cm^{-1} indicating C=C stretching in aromatic rings and C=O stretches in conjugated carbonyl systems. However, Cig-FA has a discrete sharp peak at 1639 cm^{-1} that somewhat overlaps with a broader peak around 1615 cm^{-1} (Figure 4A). This could be due to organic nitrates (R-ONO_2) that absorb in the same region but typically have sharp and discrete peaks.[31] Cig-FA, SRFA and NFA all exhibit broad peaks centered near 1388–1403 cm^{-1} indicating C-H bending from aliphatic groups (Figure 4B); interestingly, this feature was absent in Wood-FA spectra. All samples have broad peaks centered near 1195–1211 cm^{-1} that have been attributed to C=O stretching and OH bending from carboxylic acids (Figure 4B) (Kristensen et al., 2015). These FT-IR features of Cig-FA and Wood-FA are consistent with spectra of HULIS isolated from ambient PM,[24] CSC,[4] and water-soluble organic fraction of PM extracts.[4,18,21,32] However, both Cig-FA and Wood-FA have peaks that are not seen in SRFA and NFA. Both Cig-FA and Wood-FA have discrete peaks near 1512 cm^{-1} may indicate aromatic nitro compounds (C-NO_2).[31] Cig-FA shows a discrete peak near 1561 cm^{-1} that may indicate N-O stretching in organic nitro compounds (R-NO_2), although this peak is not seen in Wood-FA. Peaks centered near 1460 cm^{-1} are associated with C-H bonds from aliphatic groups. One peak centered near 1105 cm^{-1} indicates C-O bonds from aliphatic ethers (Figure 4B). The peaks centered near 1460 cm^{-1} and 1105 cm^{-1}, are not seen in SRFA and are consistent with the more aliphatic character observed in HULIS.[4,19] The peak at 1045 cm^{-1} indicates C-OH bond from primary alcohols and has been observed in urban HULIS.[33] The Cig-FA spectrum also shows a discrete sharp peak around 815 cm^{-1} that might be attributed to organic nitrates ($RONO_2$) and inorganic nitrates.[33] Cig-FA and Wood-FA fractions contain significant amounts of HULIS-bearing functional groups similar to SRFA and NFA, but with more aliphatic, organic nitro and nitrate character.

Biological effects of HULIS.

HULIS demonstrate a capacity to complex and accumulate metals, including iron. Respiratory epithelial cells exposed to the water-soluble fractions of both CSC and WSP as well as the standard FAs revealed an increased import of iron (Figure 5). Quantification of ferritin confirmed that the elevated iron concentrations following exposures to Cig-WS,

Wood-WS, SRFA, and NFA was intracellular with increases in the concentration of the storage protein (Figure 6).

The impact of cell exposures to CSC-WS, WSP-WS, SRFA, and NFA on release of pro-inflammatory mediators was quantified. Incubation of BEAS-2B cells with FAC alone either had no effect or slightly decreased cytokine release at 24 hours. IL-8 and IL-6 release by respiratory epithelial cells was increased following exposures to CSC-WS, WSP-WS, and the standard fulvic acids (Figures 7A–D and 8A–D). However, co-exposure of the respiratory epithelial cells with FAC with CSC-WS, WSP-WS, SRFA, and NFA significantly decreased supernatant concentrations of the interleukin relative to exposures to CSC-WS, WSP-WS, and the standard fulvic acids alone (Figures 7A–D and 8A–8D).

Discussion

Both fluorescence EEM spectra and FT-IR demonstrate strong similarities between a component of the water-soluble extracts of both CSC and WSP and two standard fulvic acids (SRFA and NFA). This is consistent with prior results showing HULIS, including a FA-like substance, in CSC and ambient air particles.[4,8] The fluorescence spectra of Cig-WS and Cig-FA demonstrated contours stretching into lower wavelengths relative to the spectra of SRFA. Dissimilarities could be due to the presence of lower molecular weight substances with less aromaticity and unsaturated bonds, consistent with observations of ambient HULIS extracts.[21,22] These FT-IR features of Cig-FA and Wood-FA are consistent with spectra of HULIS isolated from ambient PM,[24] CSC,[4] and water-soluble organic fraction of PM extracts.[18,21,32]

HULIS demonstrates a capacity to complex and accumulate metals, including iron. Respiratory epithelial cells exposed to the water-soluble fractions of both CSC and WSP and the standard fulvic acids revealed an increased import of iron. Quantification of ferritin confirmed that the iron was intracellular with increases in the concentration of the storage protein following exposures to CSC-WS, WSP-WS, SRFA, and NFA. In the lungs of smokers exposed to cigarette smoke particle, the concentration of iron has been shown to increase.[34] A brownish-black material with solubility properties and composition similar to HULIS can be isolated from the lungs of smokers.[35] Subsequently, it is proposed that cigarette smoke particles introduce HULIS into the human lung where it complexes metals available in the lower respiratory tract to subsequently disrupt iron homeostasis. In air pollution particles, including WSP, characterization revealed the presence of functional groups with a capacity to complex metals.[6] FT-IR shows a marked resemblance to material isolated from both CSC and air pollution particles to HULIS.[8,35] The quantity of HULIS isolated from the air pollution particles correlated with the concentrations of included metal.[8] In the respiratory tract, ambient air PM has consistently demonstrated a capacity to accumulate iron from available cell sources reflecting the particle surface’s ability to complex host iron.[9] FA-like substance in HULIS can be endocytosed. After it is moved intracellularly, cell sources of iron can be complexed by carboxylic and phenolic groups included in the FA. Despite no change in iron, the cell is deficient in available metal. Subsequently, the metal will be imported to meet the demands of the FA and the cell. A new

equilibrium is attained with higher concentrations of cell iron. Some portion of this increased metal is stored in ferritin and cell levels of this storage protein also increase.

The response to exposures to the water-soluble components of CSC and WSP included a release of pro-inflammatory mediators IL-6 and IL-8, a result that has been observed earlier with metal deficiency following cell exposures to chelators.[36–38] The observation that iron alone, as well as metal in combination with FA and FA-like substances in CSC, WSP, SRFA and NFA. resulted in lower or similar levels of pro-inflammatory mediators compared to the media alone or the FA-like substances alone suggests that the oxidant generation from free or complexed metal is not responsible for the response.

Endogenous iron, essential for host function, can be complexed by a polyanionic particle surface.[39] Comparable to other compounds with a capacity to appropriate cell iron, the response to the functional metal deficiency will include oxidative stress, cell signaling, transcription factor activation, and release of pro-inflammatory mediators.[36–44] This response can be observed following human exposure to PM which contains carbonaceous compounds.[1,45] The sequestration of iron and an associated deficiency of cell metal after exposure to the standard FA and FA-like substance in cigarette smoke and WSP can initiate pathways leading to injury and disease.[46–52] Exposure to other xenobiotic agents with an equivalent capacity to coordinate metal cations impacts a comparable inflammatory and fibrotic injury in humans.[53–55] The spectrum of lung disease following smoking and air pollution particle exposure is wide and includes inflammatory injuries; these are proposed to be associated with a functional deficiency of iron resulting after sequestration of host cell metal by the HULIS including FA.[7] Exposures to both cigarette smoke and wood smoke also increase the risk for lung fibrosis.[56–58] These associations between 1) smoking and exposures to air pollution particles and wood smoke and 2) inflammatory and fibrotic lung injuries are comparable to other exposures to other xenobiotic agents with an equivalent capacity to coordinate metal cations.

The observation of a FA-like substance in CSC-WS and WSP-WS has a specific significance. As a result of their water-solubility, FA-like substances in CSC and WSP are anticipated to permeate the blood vessels to be distributed systemically. The capacity of these substances to initiate iron sequestration in cells and tissues will impact oxidative stress, signaling, transcription factor activation, release of pro-inflammatory mediators, apoptosis, inflammation, and fibrosis in exposed cells and tissues predicting a capacity of cigarette smoke particle and WSP to initiate extra-pulmonary disease. Subsequently, it is possible that the systemic effects of smoking and WSP (e.g. coronary artery disease and cerebrovascular disease) can be explained by a systemic distribution of a FA-like substance included in the cigarette and WSP.

Conclusions

It is concluded that 1) FA-like substance is included in cigarette smoke and WSP and 2) respiratory epithelial cell exposure to this substance results in a disruption of iron homeostasis associated with both a cell deficiency of the metal and inflammatory response. The observation of a FA-like substance in Cig-WS and Wood-WS has a specific

significance. As a result of their water-solubility, FA-like substance in cigarette smoke and WSP is anticipated to permeate the blood vessels to be distributed systemically. The capacity of this substance to initiate iron sequestration in cells and tissues will impact oxidative stress, signaling, transcription factor activation, release of pro-inflammatory mediators, apoptosis, inflammation, and fibrosis in exposed cells and tissues predicting a capacity of cigarette smoke and WSP to initiate extra-pulmonary disease. Subsequently, it is possible that the systemic effects of smoking and WSP (e.g. coronary artery disease and cerebrovascular disease) can be explained by a systemic distribution of a FA-like substance included in the cigarette smoke and WSP.

Acknowledgements

We would like to thank Dr. Miguel Garcia-Garibay for allowing us to use his facilities and ATR-FTIR instrument to perform measurements. We also thank Jiaqi Shen for assistance in plotting the Excitation-Emission Matrices with MATLAB.

Funding information

This research was supported by internal funds of the United States Environmental Protection Agency.

Abbreviations

CFC	Cigarette smoke condensate
Cig-FA	Fulvic acid fraction of cigarette smoke
Cig-WS	Water-soluble components of cigarette smoke
EEM	Excitation-emission matrix
ELISA	Enzyme linked immunosorbent assay
FA	Fulvic acid
FAC	Ferric ammonium citrate
FT-IR	Fourier transform infrared
HA	Humic acid
HBSS	Hank’s buffered saline solution
ICPOES	Inductively coupled plasma optical emission spectroscopy
IL	Interleukin
IHSS	International Humic Substances Society
KGM	Keratinocyte growth medium
NFA	Nordic fulvic acid
NRF2	Nuclear factor erythroid 2-related factor 2
PM	Particulate matter

ROS	Reactive oxygen species
SRFA	Suwanee River fulvic acid
TCA	Trichloroacetic acid
Wood-FA	Fulvic acid fraction of wood smoke particle
Wood-WS	Water-soluble components of wood smoke particle
WSP	Wood smoke particle

References

(1). Ghio AJ, Stonehuerner J, & Quigley DR (1994). Humic-like substances in cigarette smoke condensate and lung tissue of smokers. American Journal of Physiology-Lung Cellular and Molecular Physiology, 266(4), L382–L388.

(2). Jacobson M, Hansson HC, Noone K, & Charlson R (2000). Organic atmospheric aerosols: Review and state of the science. Reviews of Geophysics, 38(2), 267–294.

(3). Dinar E, Mentel T, & Rudich Y (2006). The density of humic acids and humic like substances (HULIS) from fresh and aged wood burning and pollution aerosol particles. Atmospheric Chemistry and Physics, 6(12), 5213–5224.

(4). Graber E & Rudich Y (2006). Atmospheric HULIS: How humic-like are they? A comprehensive and critical review. Atmospheric Chemistry and Physics, 6(3), 729–753.

(5). Hoffer A, Gelencsér A, Guyon P, Kiss G, Schmid O, Frank G, et al. (2006). Optical properties of humic-like substances (HULIS) in biomass-burning aerosols. Atmospheric Chemistry and Physics, 6(11), 3563–3570.

(6). Forrister H, Liu J, Scheuer E, Dibb J, Ziemba L, Thornhill KL, et al. (2015). Evolution of brown carbon in wildfire plumes. Geophysical Research Letters, 42(11), 4623–4630.

(7). Ghio AJ & Madden MC (2017). Human lung injury following exposure to humic substances and humic-like substances. Environmental Geochemistry and Health, 40(2), 571–581. [PubMed: 28766124]

(8). Ghio AJ, Stonehuerner J, Pritchard RJ, Piantadosi CA, Quigley DR, Dreher KL, & Costa DL (1996). Humic-like substances in air pollution particulates correlate with concentrations of transition metals and oxidant generation. Inhalation Toxicology, 8(5), 479–494.

(9). Ghio AJ, Soukup JM, Dailey LA, Tong H, Kesic MJ, Budinger GS, & Mutlu GM (2015). Wood smoke particle sequesters cell iron to impact a biological effect. Chemical Research in Toxicology, 28(11), 2104–2111. [PubMed: 26462088]

(10). Yang R & van den Berg CM (2009). Metal complexation by humic substances in seawater. Environmental Science & Technology, 43(19), 7192–7197. [PubMed: 19848121]

(11). Yamamoto M, Nishida A, Otsuka K, Komai T, & Fukushima M (2010). Evaluation of the binding of iron (II) to humic substances derived from a compost sample by a colorimetric method using ferrozine. Bioresource Technology, 101(12), 4456–4460. [PubMed: 20163958]

(12). Town RM, Duval JFL, Buffle J, & van Leeuwen HP (2012). Chemodynamics of metal complexation by natural soft colloids: Cu (II) binding by humic acid. The Journal of Physical Chemistry A, 116(25), 6489–6496. [PubMed: 22324832]

(13). Qian M & Eaton JW (1989). Tobacco-borne siderophoric activity. Archives of Biochemistry and Biophysics, 275(1), 280–288. [PubMed: 2510603]

(14). Gonzalez DH, Cala CK, Peng Q, & Paulson SE (2017). HULIS enhancement of hydroxyl radical formation from Fe (II): Kinetics of fulvic acid-Fe (II) complexes in the presence of lung anti-oxidants. Environmental Science & Technology, 51(13), 7676–7685. [PubMed: 28581715]

(15). Paulson SE, Anastasio CC, & Hasson A (2016). Probing the intrinsic ability of particles to generate reactive oxygen species and the effect of physiologically relevant solutes. https://www.arb.ca.gov/research/apr/past/10-314-1.pdf. California ARB.

(16). Simoneit BR (1980). Eolian particulates from oceanic and rural areas—their lipids fulvic and humic acids and residual carbon. Physics and Chemistry of the Earth, 12, 343–352.

(17). Mukai H & Ambe Y (1986). Characterization of a humic acid-like brown substance in airborne particulate matter and tentative identification of its origin. Atmospheric Environment (1967), 20(5), 813–819.

(18). Havers N, Burba P, Lambert J, & Klockow D (1998). Spectroscopic characterization of humic-like substances in airborne particulate matter. Journal of Atmospheric Chemistry, 29(1), 45–54.

(19). Win MS, Tian Z, Zhao H, Xiao K, Peng J, Shang Y, et al. (2018). Atmospheric HULIS and its ability to mediate the reactive oxygen species (ROS): A review. Journal of Environmental Sciences, 71, 13–31.

(20). Leenheer JA & Croué J-P (2003). Peer reviewed: characterizing aquatic dissolved organic matter. Environmental Science & Technology, 37(1), 18A–26A.

(21). Krivacsy Z, Kiss G, Varga B, Galambos I, Sárvári Z, Gelencser A, et al. (2000). Study of humic-like substances in fog and interstitial aerosol by size-exclusion chromatography and capillary electrophoresis. Atmospheric Environment, 34 (25), 4273–4281.

(22). Duarte RM, Pio CA, & Duarte AC (2005). Spectroscopic study of the water-soluble organic matter isolated from atmospheric aerosols collected under different atmospheric conditions. Analytica Chimica Acta, 530(1), 7–14.

(23). Salma I, Ocskay R, Chi X, & Maenhaut W (2007). Sampling artefacts, concentration and chemical composition of fine water-soluble organic carbon and humic-like substances in a continental urban atmospheric environment. Atmospheric Environment, 41(19), 4106–4118.

(24). Kristensen TB, Du L, Nguyen QT, Nøjgaard J, Koch CB, Nielsen OF, et al. (2015). Chemical properties of HULIS from three different environments. Journal of Atmospheric Chemistry, 72(1), 65–80.

(25). Wei J, Yu H, Wang Y, & Verma V (2018). Complexation of iron and copper in ambient particulate matter and its effect on the oxidative potential measured in a surrogate lung fluid. Environmental Science & Technology, 53(3), 1661–1671.

(26). Yu H, Wei J, Cheng Y, Subedi K, & Verma V (2018). Synergistic and antagonistic interactions among the particulate matter components in generating reactive oxygen species based on the dithiothreitol assay. Environmental Science & Technology, 52(4), 2261–2270. [PubMed: 29351719]

(27). Elmenhorst H (1966). A completely automatic smoking machine for the preparation of a large quantity of cigarette smoke condensate. Beier Tabakforschung, 3, 545–553.

(28). Birch M & Cary R (1996). Elemental carbon-based method for monitoring occupational exposures to particulate diesel exhaust. Aerosol Science and Technology, 25(3), 221–241.

(29). Schauer JJ, Kleeman MJ, Cass GR, & Simoneit BR (2001). Measurement of emissions from air pollution sources. 3. C1− C29 organic compounds from fireplace combustion of wood. Environmental Science & Technology, 35(9), 1716–1728. [PubMed: 11355184]

(30). Andersen CM & Bro R (2003). Practical aspects of PARAFAC modeling of fluorescence excitation-emission data. Journal of Chemometrics: A Journal of the Chemometrics Society, 17, (4), 200–215.

(31). Garnes LA & Allen DT (2002). Size distributions of organonitrates in ambient aerosol collected in Houston, Texas. Aerosol Science & Technology, 36(10), 983–992.

(32). Kiss G, Varga B, Galambos I, & Ganszky I (2002). Characterization of water-soluble organic matter isolated from atmospheric fine aerosol. Journal of Geophysical Research: Atmospheres, 107(D21), ICC 1–1–ICC 1–8.

(33). Chen Q, Ikemori F, Higo H, Asakawa D, & Mochida M (2016). Chemical structural characteristics of HULIS and other fractionated organic matter in urban aerosols: results from mass spectral and FT-IR analysis. Environmental Science & Technology, 50(4), 1721–1730. [PubMed: 26771766]

(34). McGowan SE, Murray JJ, & Parrish MG (1986). Iron binding, internalization, and fate in human alveolar macrophages. Translational Research, 108(6), 587–595.

(35). Ghio AJ, Jaskot RH, & Hatch GE (1994). Lung injury after silica instillation is associated with an accumulation of iron in rats. American Journal of Physiology-Lung Cellular and Molecular Physiology, 267(6), L686–L692.

(36). Laughton MJ, Moroney MA, Hoult J, & Halliwell B (1989). Effects of desferrioxamine on eicosanoid production in two intact cell systems. Biochemical Pharmacology, 38(1), 189–193. [PubMed: 2491945]

(37). Tanji K; Imaizumi T; Matsumiya T; Itaya H; Fujimoto K; Cui X; Toki T; Ito E; Yoshida H; Wakabayashi K; Satoh K, Desferrioxamine, an iron chelator, upregulates cyclooxygenase-2 expression and prostaglandin production in a human macrophage cell line. Biochim Biophys Acta 2001, 1530, (2–3), 227–35. [PubMed: 11239825]

(38). Markel TA, Crisostomo PR, Wang M, Herring CM, Lahm T, Meldrum KK, et al. (2007). Iron chelation acutely stimulates fetal human intestinal cell production of IL-6 and VEGF while decreasing HGF: the roles of p38, ERK, and JNK MAPK signaling. American Journal of Physiology-Gastrointestinal and Liver Physiology, 292(4), G958–G963. [PubMed: 17204543]

(39). Ghio AJ, Tong H, Soukup JM, Dailey LA, Cheng W-Y, Samet JM, et al. (2013). Sequestration of mitochondrial iron by silica particle initiates a biological effect. American Journal of Physiology-Lung Cellular and Molecular Physiology, 305(10), L712–L724. [PubMed: 23997175]

(40). Hileti D, Panayiotidis P, & Hoffbrand AV (1995). Iron chelators induce apoptosis in proliferating cells. British Journal of Haematology, 89(1), 181–187. [PubMed: 7833261]

(41). Kim B-S, Yoon K-H, Oh H-M, Choi E-Y, Kim S-W, Han W-C, et al. (2002). Involvement of p38 MAP kinase during iron chelator-mediated apoptotic cell death. Cellular immunology, 220(2), 96–106. [PubMed: 12657244]

(42). Lee S-K, Jang H-J, Lee H-J, Lee J, Jeon B-H, Jun C-D, et al. (2006). p38 and ERK MAP kinase mediates iron chelator-induced apoptosis and-suppressed differentiation of immortalized and malignant human oral keratinocytes. Life Sciences, 79(15), 1419–1427. [PubMed: 16697418]

(43). Huang X, Dai J, Huang C, Zhang Q, Bhanot O, & Pelle E (2007). Deferoxamine synergistically enhances iron-mediated AP-1 activation: a showcase of the interplay between extracellular-signal-regulated kinase and tyrosine phosphatase. Free Radical Research, 41(10), 1135–1142. [PubMed: 17886035]

(44). Liu Y, Cui Y, Shi M, Zhang Q, Wang Q, & Chen X (2014). Deferoxamine promotes MDA-MB-231 cell migration and invasion through increased ROS-dependent HIF-1α accumulation. Cellular Physiology and Biochemistry, 33(4), 1036–1046. [PubMed: 24732598]

(45). Sporn TA & Roggli VL (2008). Pneumoconioses, mineral and vegetable. In Dail and Hammar's Pulmonary Pathology, Springer, 911–949.

(46). Gau R-J, Yang H-L, Suen J-L, & Lu F-J (2001). Induction of oxidative stress by humic acid through increasing intracellular iron: a possible mechanism leading to atherothrombotic vascular disorder in blackfoot disease. Biochemical and Biophysical Research Communications, 283(4), 743–749. [PubMed: 11350046]

(47). Hseu Y-C, Huang H-W, Wang S-Y, Chen H-Y, Lu F-J, Gau R-J, & Yang H-L (2002). Humic acid induces apoptosis in human endothelial cells. Toxicology and Applied Pharmacology, 182(1), 34–43. [PubMed: 12127261]

(48). Cheng M-L, Ho H-Y, Huang Y-W, Lu F-J, & Chiu DT (2003). Humic acid induces oxidative DNA damage, growth retardation, and apoptosis in human primary fibroblasts. Experimental Biology and Medicine, 228(4), 413–423. [PubMed: 12671186]

(49). Yang H-L, Hseu Y-C, Hseu Y-T, Lu F-J, Lin E, & Lai J-S (2004). Humic acid induces apoptosis in human premyelocytic leukemia HL-60 cells. Life Sciences, 75(15), 1817–1831. [PubMed: 15302226]

(50). Hseu Y-C, Kumar KS, Chen C-S, Cho H-J, Lin S-W, Shen P-C, et al. (2014). Humic acid in drinking well water induces inflammation through reactive oxygen species generation and activation of nuclear factor-κB/activator protein-1 signaling pathways: a possible role in atherosclerosis. Toxicology and Applied Pharmacology, 274(2), 249–262. [PubMed: 24239652]

(51). van Eijl S, Mortaz E, Ferreira AF, Kuper F, Nijkamp FP, Folkerts G, & Bloksma N (2011). Humic acid enhances cigarette smoke-induced lung emphysema in mice and IL-8 release of human monocytes. Pulmonary Pharmacology & Therapeutics, 24(6), 682–689. [PubMed: 21820074]

(52). Hseu Y-C, Lin E, Chen JY, Liua YR, Huang CY, Lu FJ, et al. (2009). Humic acid induces G1 phase arrest and apoptosis in cultured vascular smooth muscle cells. Environmental Toxicology: An International Journal, 24(3), 243–258.

(53). Løvstad RA (1991). The reaction of ferric-and ferrous salts with bleomycin. The International Journal of Biochemistry, 23(2), 235–238. [PubMed: 1705524]

(54). Ueda N, Guidet B, & Shah SV (1993). Gentamicin-induced mobilization of iron from renal cortical mitochondria. American Journal of Physiology-Renal Physiology, 265(3), F435–F439.

(55). Elias Z, Poirot O, Danière M-C, Terzetti F, Binet S, Tomatis M, & Fubini B (2002). Surface reactivity, cytotoxicity, and transforming potency of iron-covered compared to untreated refractory ceramic fibers. Journal of Toxicology and Environmental Health Part A, 65(23), 2007–2027. [PubMed: 12490045]

(56). Kitamura H, Ichinose S, Hosoya T, Ando T, Ikushima S, Oritsu M, & Takemura T (2007). Inhalation of inorganic particles as a risk factor for idiopathic pulmonary fibrosis—elemental microanalysis of pulmonary lymph nodes obtained at autopsy cases. Pathology-Research and Practice, 203(8), 575–585

(57). Mullen J, Hodgson MJ, DeGraff AC, & Godar T (1998). Case-control study of idiopathic pulmonary fibrosis and environmental exposures. Journal of Occupational and Environmental Medicine, 40(4), 363–367. [PubMed: 9571528]

(58). Taskar V & Coultas D (2008). Exposures and idiopathic lung disease. Seminars in Respiratory and Critical Care Medicine, 29(6), 670–9. [PubMed: 19221965]

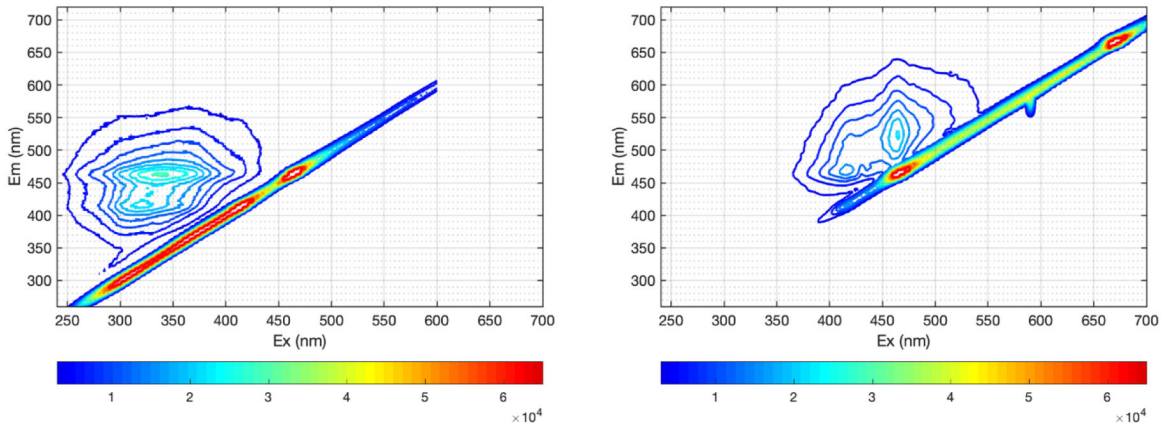

Figure 1.
Fluorescence EEM of SRFA (Standard II) (left) and NFA (right) in H_2O (pH 5.5).

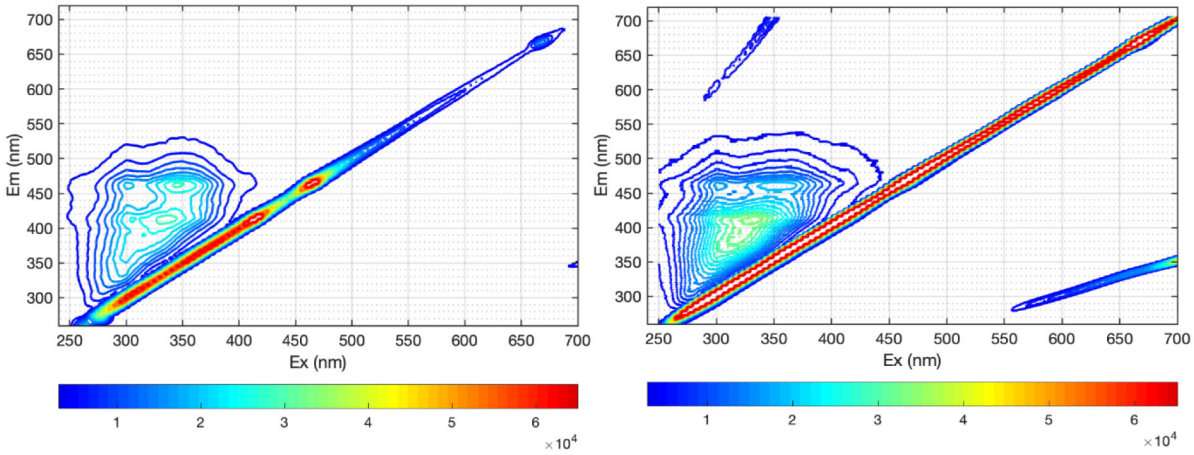

Figure 2.
Fluorescence EEM of Cig-WS (left) and Cig-FA (right).

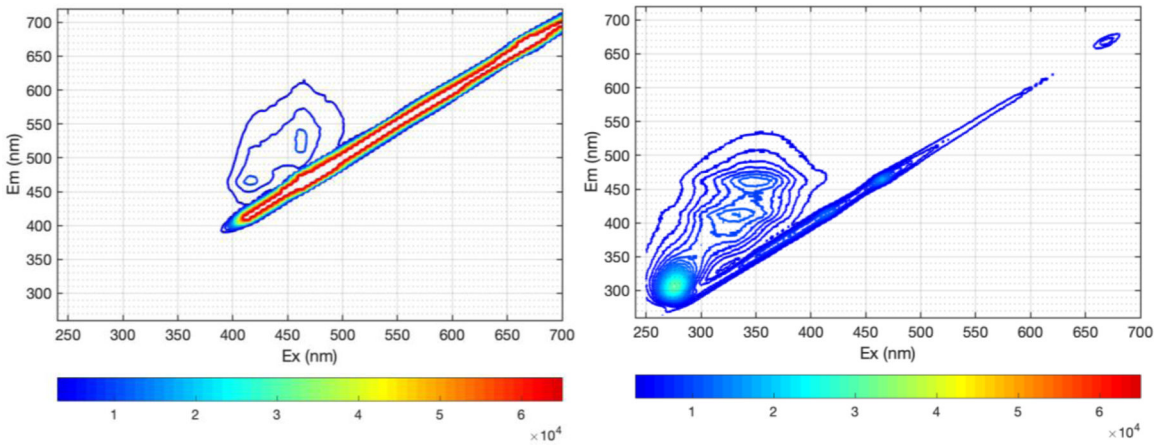

Figure 3.
Fluorescence EEM of Wood-WS (left) and Wood-FA (right).

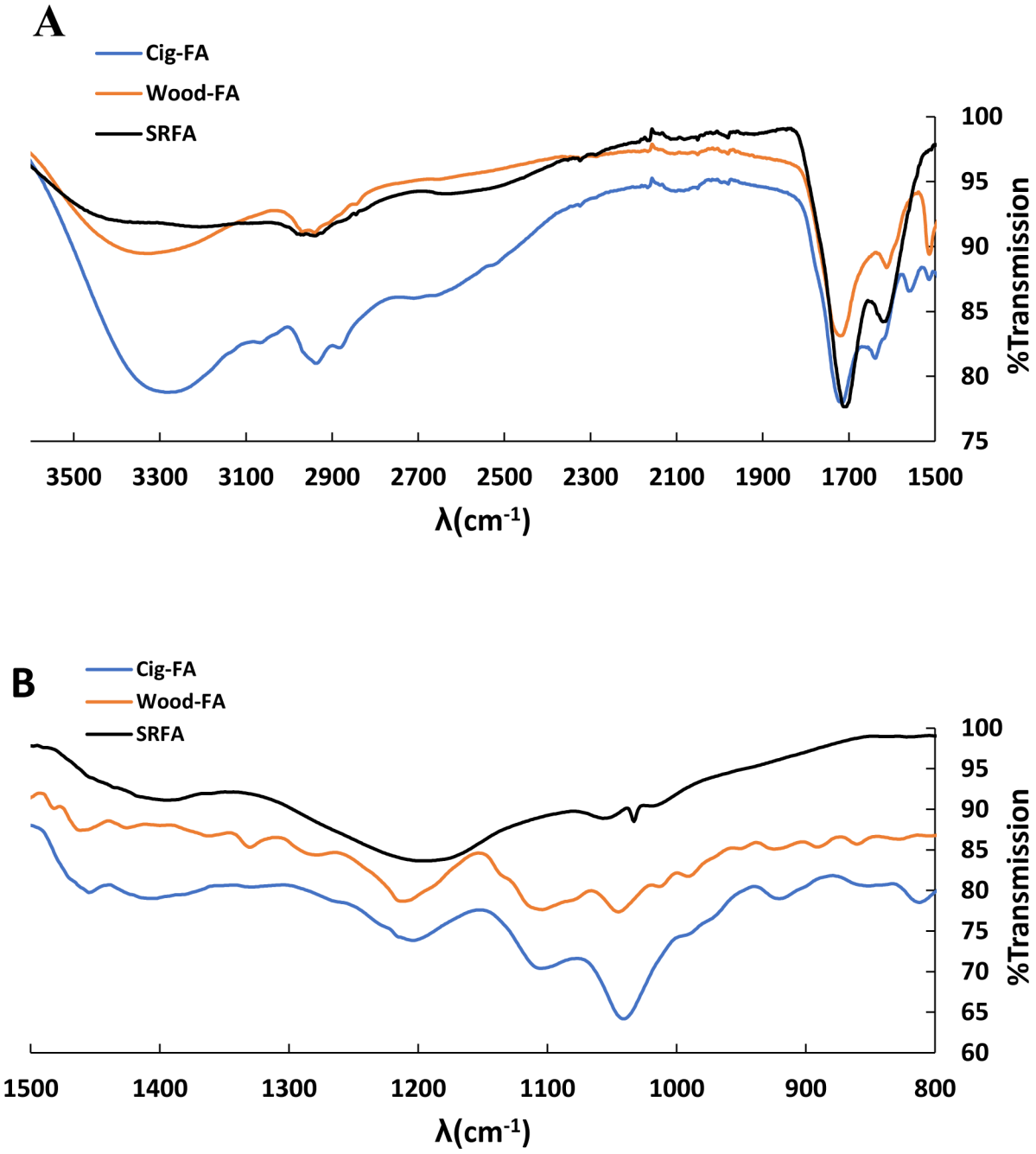

Figure 4.
FTIR Spectra of Wood-FA, Cig-FA, and SRFA.

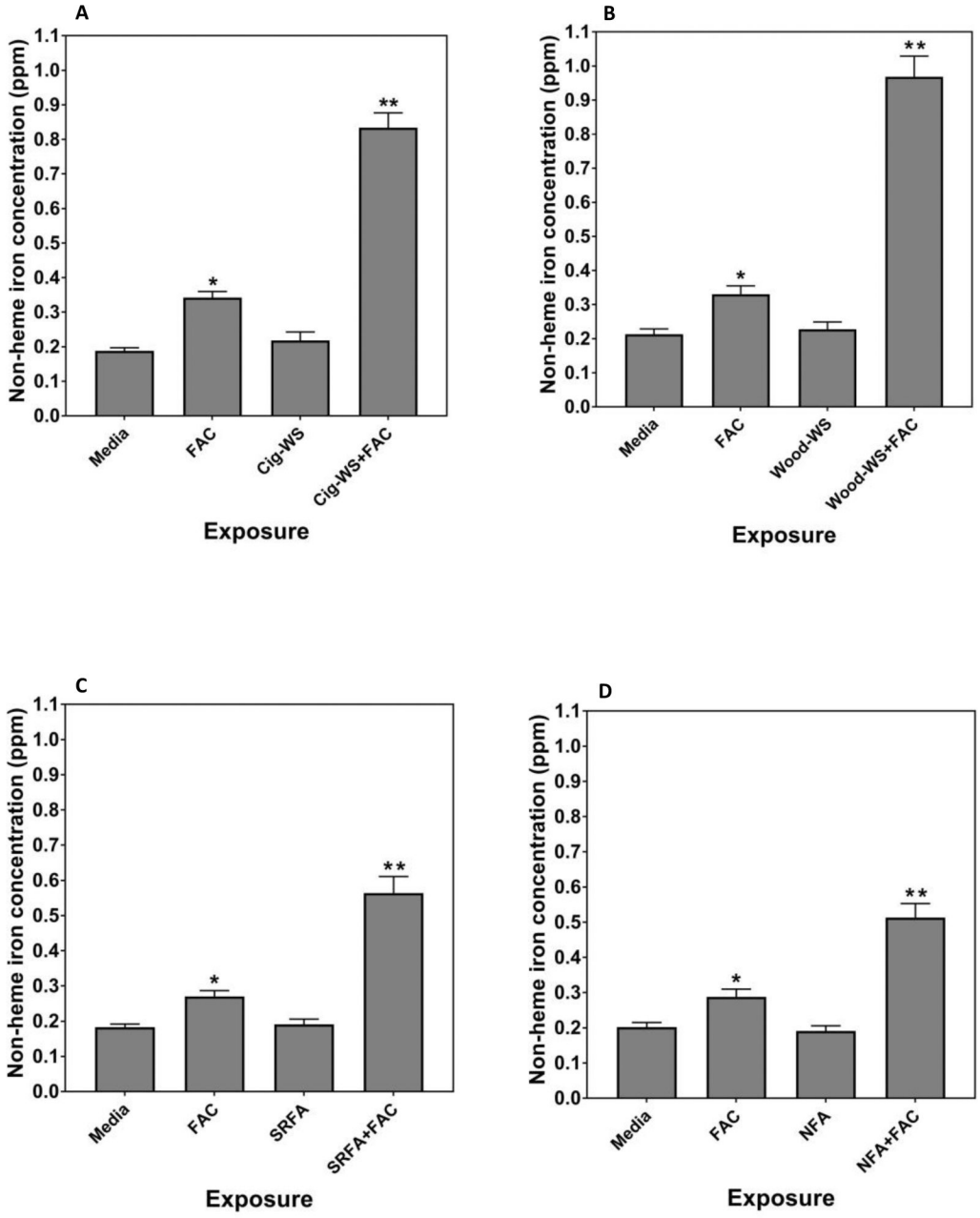

Figure 5.

Cell non-heme iron concentrations following 4 hr exposures of BEAS-2B cells to media, 200 μM FAC, 100 μL Cig-WS, and both Cig-WS and FAC (A). Exposure to FAC increased cell non-heme iron but co-exposure of Cig-WS with FAC was associated with significantly increased non-heme iron concentrations. Similarly, co-exposures of 100 μL Wood-WS (B), 100 μg/mL SRFA (C), and 100 μg/mL NFA (D) with FAC significantly elevated cell non-heme iron concentrations.

* indicates a significant increase relative to exposure of BEAS-2B cells to media only while ** indicates a significant increase relative to all other exposures.

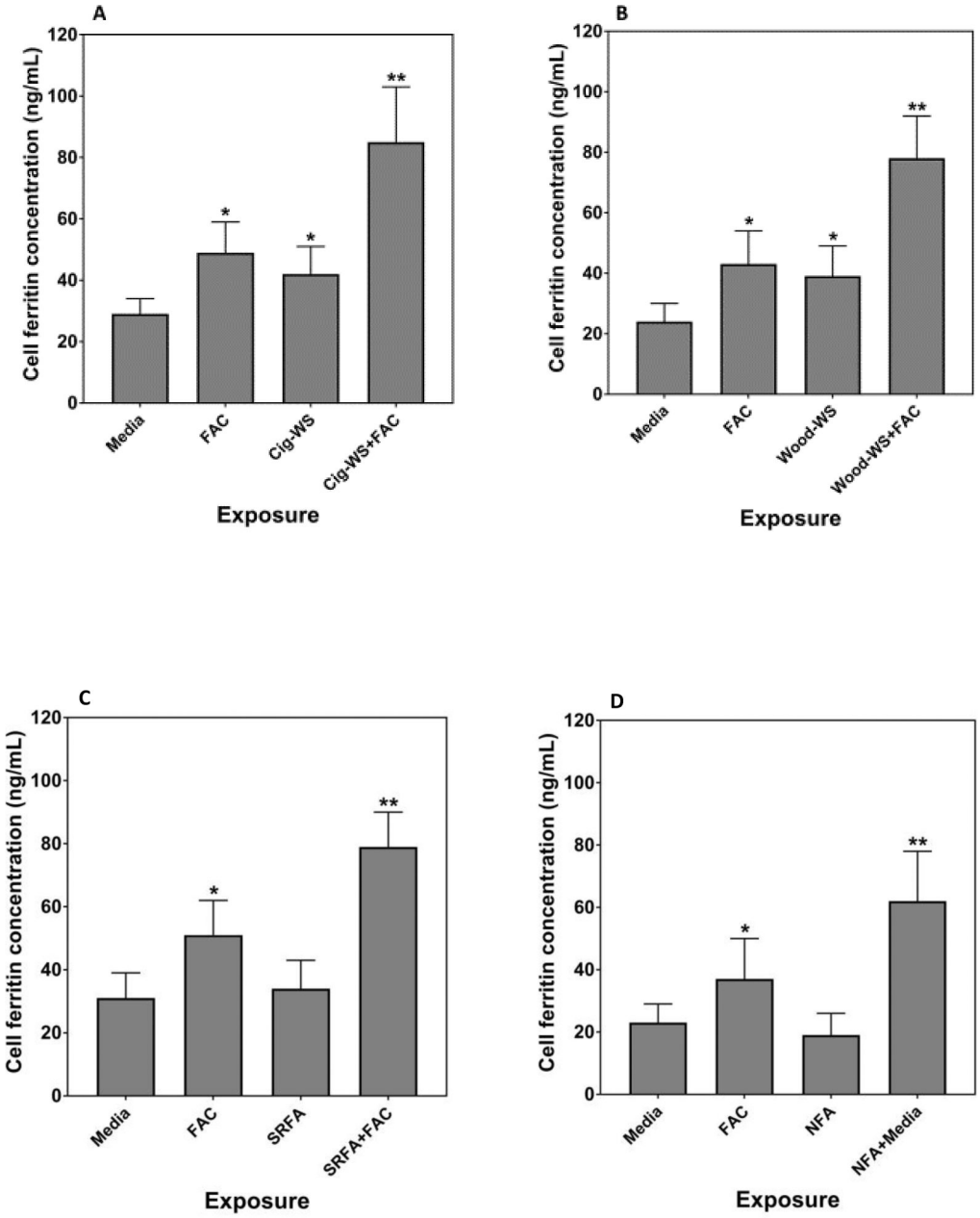

Figure 6.

Cell ferritin concentrations following 24 hr exposures of BEAS-2B cells to media, 200 μM FAC, 100 μL Cig-WS, and both Cig-WS and FAC (A). Exposures to FAC only and Cig-WS only both increased cell ferritin levels but co-exposure of Cig-WS with FAC was associated with significantly increased cell ferritin concentrations. Similarly, co-exposures of 100 μL Wood-WS (B), 100 μg/mL SRFA (C), and 100 μg/mL NFA (D) with FAC significantly elevated cell ferritin concentrations. Unlike incubations with Cig-WS only (A) and Wood-WS only (B), those with SRFA only (C) and NFA only (D) did not impact cell ferritin.
* indicates a significant increase relative to exposure of BEAS-2B cells to media only while ** indicates a significant increase relative to all other exposures.

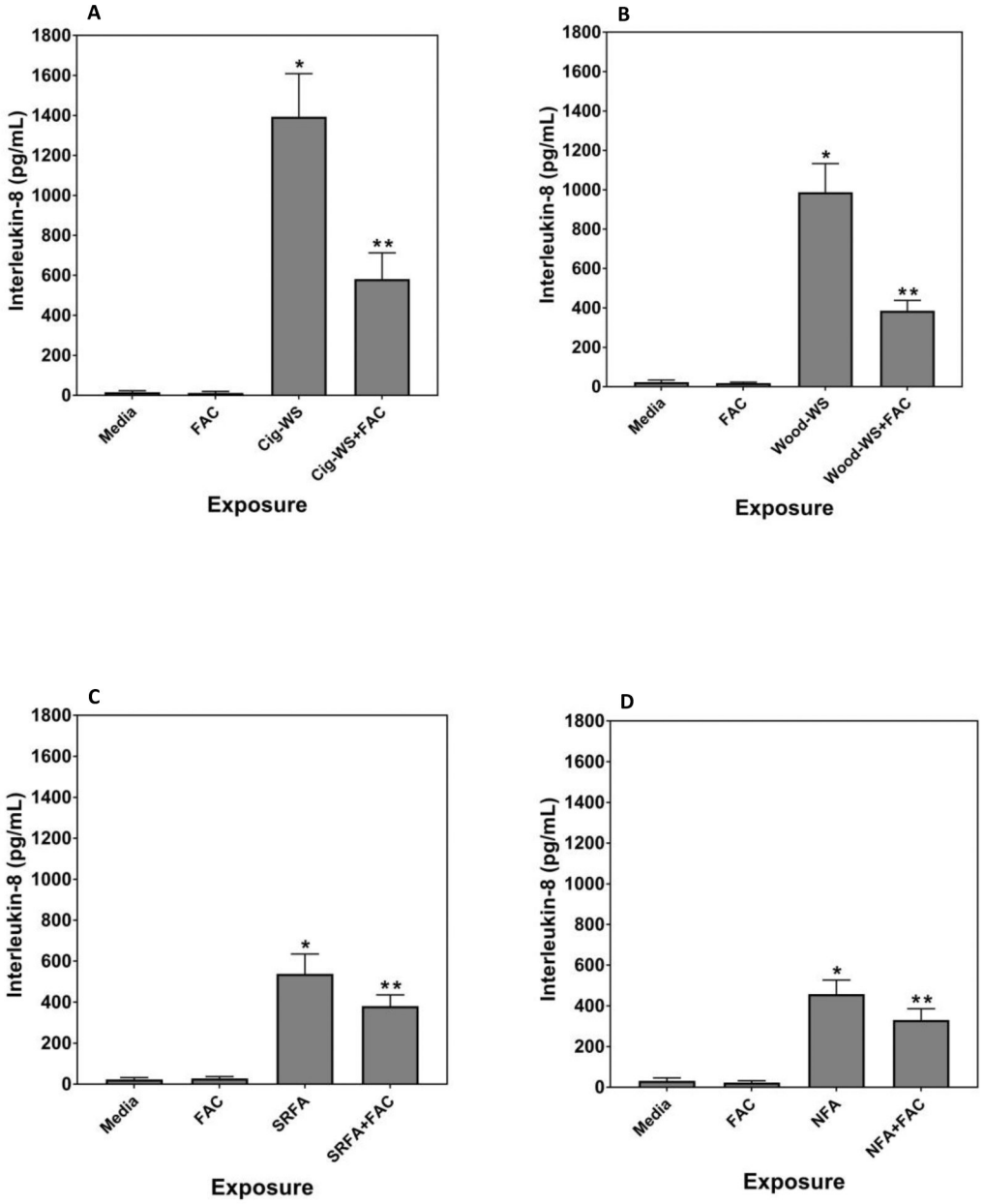

Figure 7.

Release of IL-8 after 24 hr exposure of BEAS-2B cells to Cig-WS (A), Wood-WS (B), SRFA (C), and NFA (D) with and without FAC included in the incubation. Exposure to Cig-WS, Wood-WS, SRFA, and NFA all significantly increased the release of IL-8 and IL-6. FAC treatment significantly diminished this response.

* indicates a significant increase relative to all other exposures, and ** indicates a significant increase relative to media exposure.

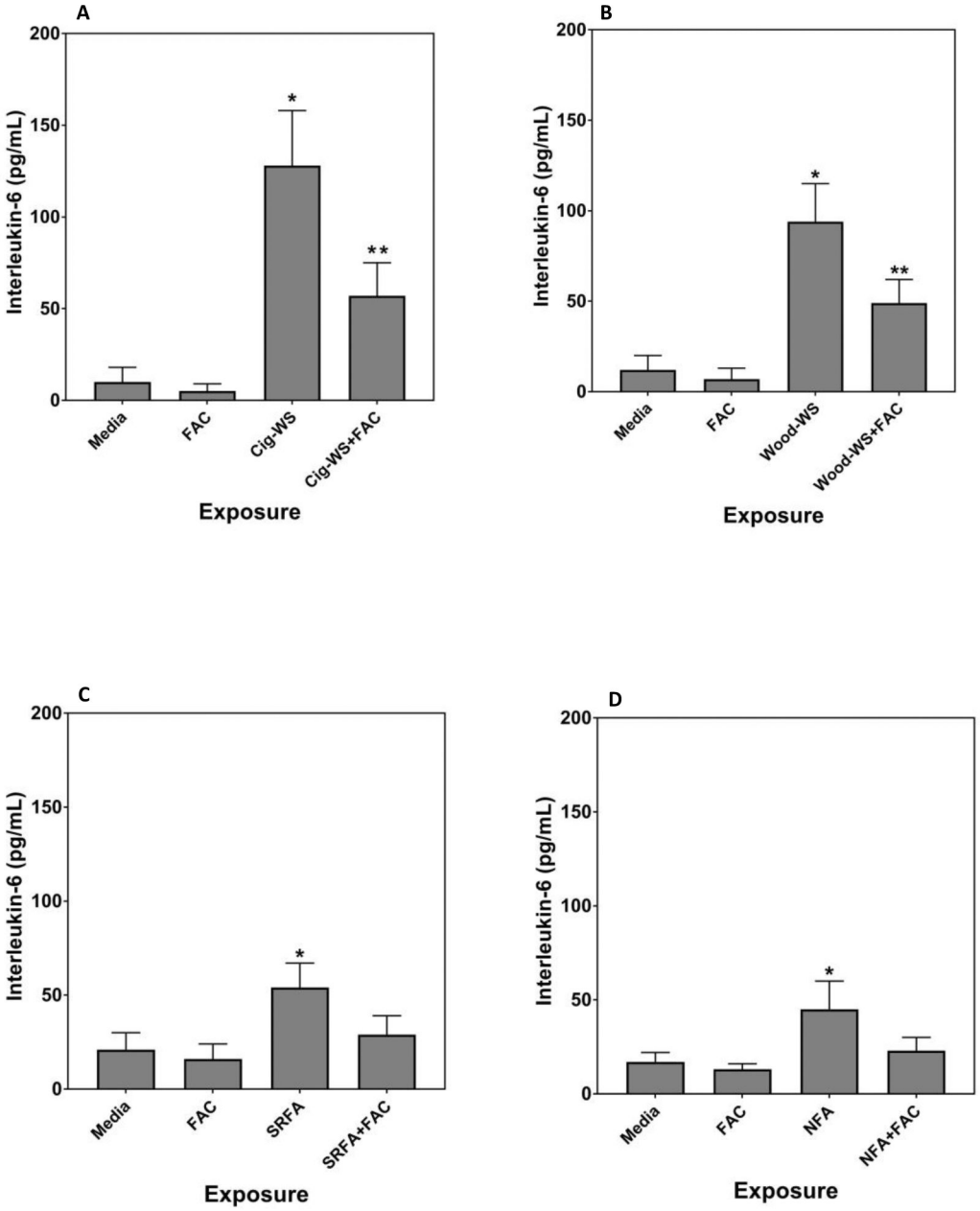

Figure 8.

Release of IL-6 after 24 hr exposure of BEAS-2B cells to Cig-WS (A), Wood-WS (B), SRFA (C), and NFA (D) with and without FAC included in the incubation. Exposure to Cig-WS, Wood-WS, SRFA, and NFA all significantly increased the release of IL-8 and IL-6. FAC treatment significantly decreased this response.

* indicates a significant increase relative to all other exposures, and ** indicates a significant increase relative to media exposure

Table 1.

Summary of common FTIR peaks among samples.

SRFA	Nordic FA*	Cig-FA	Wood-FA	Bond	Functional Group
3308	3398	3280	3333	O-H	Alcohols, phenols, carboxylic acids
2938	2975	2937	2950	C-H	Aliphatic
1707	1723	1715	1720	C=O	Carboxylic acids, ketones, aldehydes
1620	1620	1639	1611	C=C C=O	Aromatic and conjugated systems
1398	1388	1403		C-H	Alkane
1195	1208	1204	1211	C-O	Esters